Malaysian Journal of Chemistry, 2026, Vol. 28(1), 9-19
(Special Issue: *3rd International Conference on Industry-Academia Initiatives in Biotechnology & Chemistry, iCIABC2025*)

Study on the Electrical Properties in Modified Alginate-PVA Polymer Electrolytes Doped Ammonium Thiocyanate

Nurul Aqilah Abdul Wahab[1], Noor Saadiah Mohd Ali[1,2] and Ahmad Salihin Samsudin[1]*
[1]Ionic Materials Team, Faculty of Industrial Sciences & Technology, Universiti Malaysia Pahang Sultan Abdullah, 26300 Kuantan, Pahang, Malaysia
[2]Department of Chemistry, Centre for Foundation Studies, International Islamic University Malaysia, 26300 Gambang, Pahang, Malaysia
*Corresponding author (e-mail: ahmadsalihin@umpsa.edu.my)

The increasing interest in green energy storage materials for electrochemical devices, with the development of bio-polymer materials as electrolyte candidates, has attracted significant attention recently. It can offer many high-value opportunities, provided that lower costs can be achieved, while remaining environmentally friendly. The current study emphasizes on the electrical and conduction properties of the solid bio-polymer electrolytes (SBPE) based on alginate (Alg) and polyvinyl alcohol (PVA) blend doped with different weight percentages (wt.%) of ammonium thiocyanate (NH_4SCN). SBPE samples were successfully prepared via solution casting. The impedance studies demonstrate a reduction in R_b value with NH_4SCN content up to 35 wt.%, corresponding to the highest ionic conductivity at room temperature of 3.4 (10^{-4} S cm^{-1}). In temperature-dependent studies, SBPE systems follow Arrhenius behaviour, where the regression value approaches 1. Optimum ionic conductivity has been examined to fit the complex dielectric permittivity, dielectric loss, and complex conductivity. The dielectric behavior of the Alginate-PVA-NH_4SCN SBPEs system was measured using complex permittivity and complex electrical modulus. This also shows non-Debye behavior, where no single relaxation was found in the present SBPE system. The finding suggests the great potential of Alg-PVA-NH_4SCN SBPEs as electrolytes for practical applications, such as proton batteries and supercapacitors.

Keywords: Ammonium thiocyanate, electrical, ionic conductivity, intermolecular interaction

Received: May 2025; Accepted: November 2025

In recent advancements within the battery industry, solid biopolymer electrolyte (SBPE) systems have emerged as a promising alternative due to their environmentally benign characteristics. Biopolymers—naturally derived, biodegradable macromolecules synthesized from waste-derived materials—have garnered significant attention as host matrices in the development of proton-conducting SBPEs. Their inherent safety, sustainability, and cost-effectiveness render them ideal candidates for large-scale energy storage applications [1]. Various biopolymers have been investigated for this purpose, including carboxymethyl cellulose (CMC) [2–4], chitosan [5–7], cornstarch [8], and 2-hydroxyethyl cellulose (2-HEC) [9], owing to their favorable physicochemical and electrochemical properties.

In recent years, numerous bio-derived materials such as carboxymethyl cellulose (CMC), chitosan, starch, and carrageenan [3] have been explored for their potential in electrochemical applications. SBPEs have demonstrated promising properties as solid-state electrolytes, notably being solvent-free and exhibiting no leakage. Consequently, significant research efforts have been directed toward the formulation of biopolymer electrolytes by combining natural polymers with appropriate ionic dopants. In the present study, alginate has been employed as the host biopolymer. Alginate is an anionic polysaccharide extracted from the cell walls of brown algae, composed of linear binary copolymers consisting of (1→4)-linked β-D-mannuronic acid (M) and α-L-guluronic acid (G) residues. These monomers are arranged in homopolymeric (M or G) and heteropolymeric (MG) block sequences [4]. Alginate also exhibits favorable adhesive properties and inherently low toxicity, making it a suitable candidate for bio-electrolyte systems.

Recent research has shown that doping biopolymer matrices with suitable salts can improve ionic conductivity and dielectric performance by increasing charge carrier concentration and reducing ion association [1]. Among potential ionic dopants, Ammonium Thiocyanate offers greater ionic dissociation, which can enhance charge-transport properties in polymer matrices [2]. However, its specific impact on AC conduction mechanisms, dielectric behavior, and relaxation time in Alginate-PVA-based SBPEs has not been extensively explored. A systematic investigation into the interplay between conductivity, dielectric response, and relaxation dynamics is necessary to bridge this knowledge gap.

†Paper presented at the 3rd International Conference on Industry-Academia Initiatives in Biotechnology & Chemistry

One of the major obstacles in SBPE development is the limited understanding of electrical properties, particularly in terms of AC conduction and dielectric behavior. Ionic transport in SBPEs is significantly influenced by factors such as polymer segmental motion, ion-polymer interactions, and charge carrier mobility, all of which are governed by frequency and temperature-dependent conduction mechanisms [3]. Dielectric permittivity and loss further determine charge storage capabilities and polarization effects within the system. However, many studies focus primarily on enhancing ionic conductivity without adequately addressing the fundamental dielectric and relaxation characteristics that influence charge transport dynamics [4]. A deeper understanding of these properties is essential for optimizing SBPE performance in practical applications.

Table 1. Content of Alg-PVA-NH_4SCN.

Sample designation	*NH_4SCN (wt.%)*	*NH_4SCN (g)*
APN1	5	0.1052
APN2	10	0.2222
APN3	15	0.3529
APN4	20	0.5000
APN5	25	0.6667
APN6	30	0.8571
APN7	35	1.0769
APN8	40	1.3333
APN9	45	1.6363

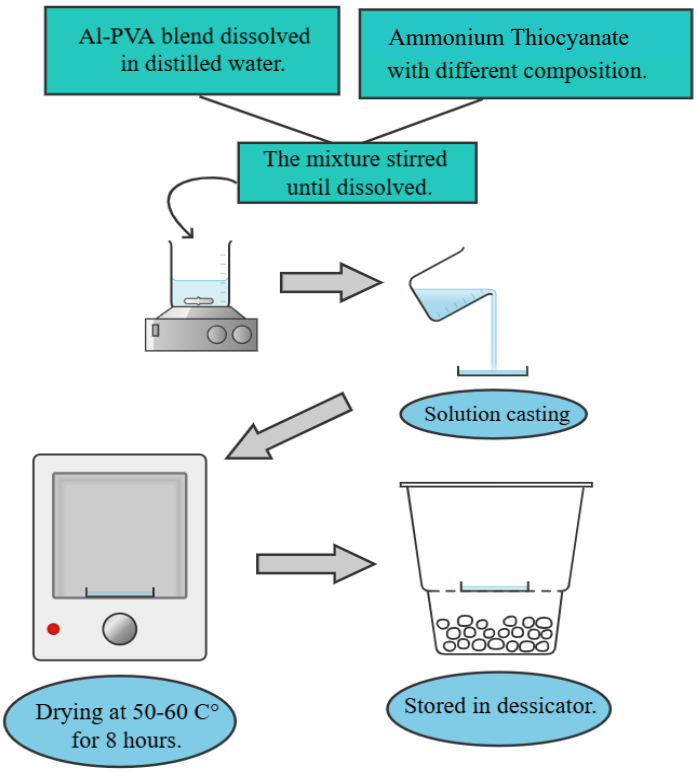

Figure 1. Sample preparation [5].

EXPERIMENTAL

Chemicals and Materials

Using the solution-casting method, the SBPE system was developed with NH_4SCN as the ionic dopant and alginate-PVA polymer blends as the host matrix. After dissolving 0.6 g of pure PVA (Merck Schuchardt, average molecular weight of 70,000 g/mol, 85% hydrolyzed) and 1.40 g of sodium alginate (Sigma Aldrich, average molecular weight of 216.12 $gmol^{-1}$) in distilled water, they were doped with different weight percentages of NH_4SCN (ranging from 5 to 40 wt.%) while being continuously stirred until they were completely dissolved. The liquid was cast into a petri dish and dried in a vacuum oven at 55–60 °C until a dry solid-film had fully formed. The sample preparation is depicted in Figure 1[5]. The content of the salt and polymer blend is tabulated in Table 1.

Characterization Methods

The immittance response properties of the SBPEs was characterized via 3532-50 LCR Hi-TESTER (HIOKI) in a controlled environment. The electrolyte films were cut into semicircles and placed on a sample holder in between two stainless steel (SS) electrodes, and impedance data were obtained for frequencies ranging from 50 Hz to 1 MHz. Analyzing an electrolyte substance's dielectric constant can help one understand its ionic conductivity whereas the dielectric studies of SBPEs offer important insights into the influence of polarization on the behavior of the electrode-electrolyte interface [6]. The determination of the AC conductivity (σ_{ac}), real part (ε_r), imaginary part (ε_i), electric modulus, ion hopping mechanism and tangent loss (δ) of dielectric permittivity were adopted from previous studies [10].

RESULTS AND DISCUSSION

Conductivity Study

The ionic conductivity derived from the EIS data was plotted against the frequency in **Figure 2**. From the results, σ increases with increasing temperature for all SBPE samples. As the temperature increases, the kinetic energy of the polymer molecules increases, leading to enhanced molecular motion. This increased energy helps break bonds and disrupt weak interactions between the oxygen atoms of alginate and PVA, and between the oxygen atoms and $^{+}$ cations. Consequently, the polymer structure becomes more flexible, reducing segmental barriers and promoting the movement of charge carriers. This leads to an increase in ionic mobility and conductivity, as ions can move more freely through the polymer matrix, facilitating better charge transport [8]. Furthermore, the conductivity of the SBPE film increases with increasing NH_4SCN content. The sudden drop in conductivity at 366 K is possibly due to ion pairing or ion aggregation, which is the temperature limit of the system amplitude. From Figure 2, it is evident that APN7 exhibits the highest ionic conductivity of 6.8×10^{-5} S cm^{-1} at ambient temperature. Additionally, the SBPEs follow the Arrhenius behavior, indicating that their ionic conductivity is thermally activated, consistent with the Arrhenius equation [12].

Table 2. Summary table of conductivity values for SBPE systems.

Sample	Conductivity (S cm^{-1})	NH4SCN content (wt.%)
APN1	5.58×10^{-8}	5
APN2	3.46×10^{-7}	10
APN3	2.10×10^{-6}	15
APN4	7.21×10^{-6}	20
APN5	2.73×10^{-5}	25
APN6	3.31×10^{-5}	30
APN7	6.80×10^{-5}	35
APN8	1.02×10^{-5}	40
APN9	5.12×10^{-6}	45

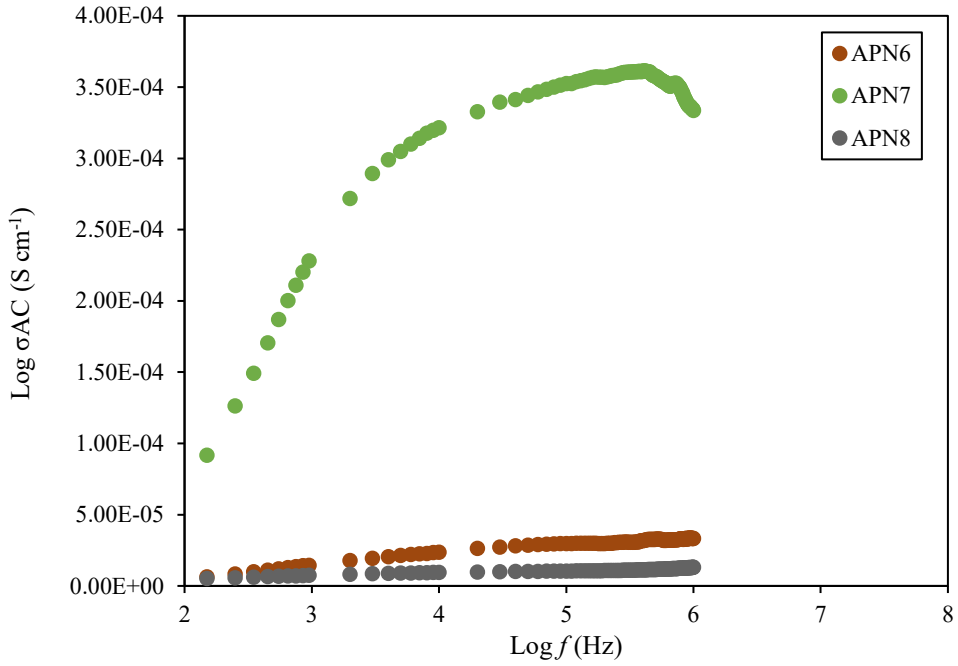

Figure 2. Frequency Dependence Conductivity for the samples at the different composition of NH_4SCN.

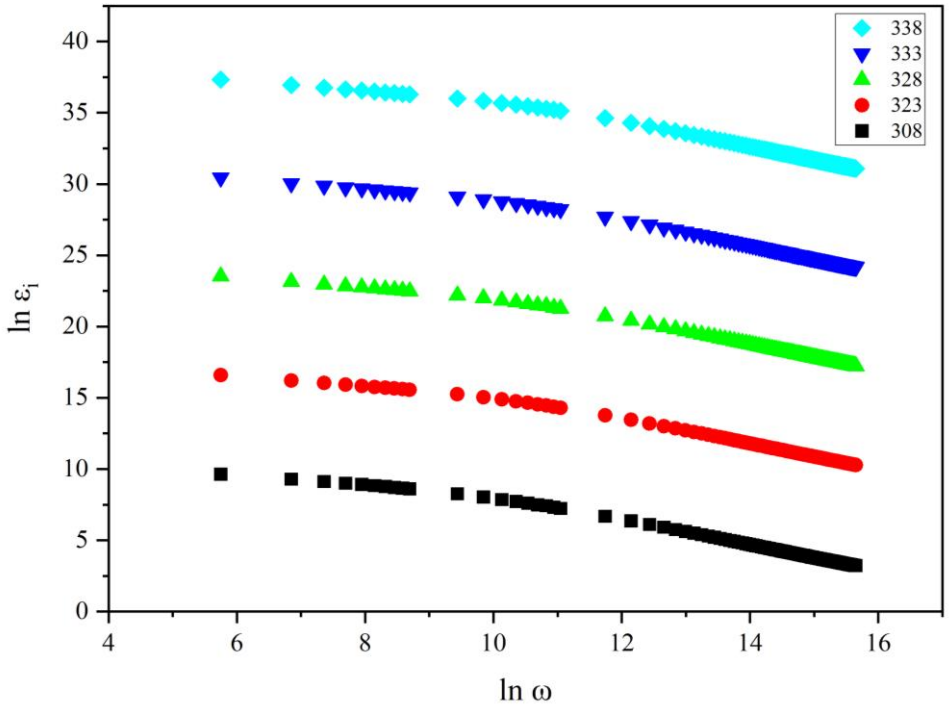

Figure 3. Plot of AC Conductivity, ε_i, against ln ω (Hz) for selected temperature of APN7.

Changes of AC Conductivity with Temperature and Ionic Conduction Mechanism

Based on equations (1) and (2), the AC conductivity (σac) of a film is determined, where the total conductivity (σ(ω)) consists of frequency-dependent log AC conductivity (σac) and frequency-independent DC conductivity (σdc). The AC conductivity follows the power law, expressed as $A\omega^s$, where A is a temperature-dependent parameter and s is the power law exponent. Additionally, temperature influences conductivity behavior. To investigate the AC conductivity mechanism in Alg-PVA-based NH_4SCN, the conductivity spectra of the optimized sample

(APN7) were analyzed over a temperature range of 303 K to 393 K. Figure 4 shows the frequency-dependent conductivity behavior, revealing distinct trends that provide insights into the ion transport mechanism and allow the frequency exponent (s) at different temperatures. Ionic conduction mechanism of the SBPEs can be achieved by using Jonscher's universal power law:

$$\sigma(\omega) = \sigma_{ac} + \sigma_{dc} \quad (1)$$

$$\sigma(\omega) = A\omega^{s} + \sigma_{dc} \quad (2)$$

These dynamics were analyzed using the Universal Power Law, which identifies the principles of conduction mechanisms.[9]. The equation used to determine the AC conductivity mechanism is as follows:

$$\sigma_{ac} = \varepsilon_0 \varepsilon'' \omega \quad (3)$$

By substituting $\sigma_{ac} = A\omega^{s}$ into Eq. 3 the value of exponent s was achieved by plotting the following equation:

$$ln\, \varepsilon_i = \frac{ln\, A}{\varepsilon_\circ} + (s-1)\, ln\, \omega \quad (4)$$

The slope of the ln ε_i plots, as shown in **Figure 3**, was utilized to determine the exponent values, which play a crucial role in understanding the material's conduction behavior. To gain deeper insight into the system's characteristics and implications, the study examines the allowable frequency range, represented as 15.4 < ln ω < 15.6. In the high-frequency region, the system exhibits different polarization effects at the electrode interface. Here, the electrode may be fully polarized, indicating a saturation in charge accumulation, or partially polarized, where charge displacement still occurs but with limited accumulation. This polarization behavior significantly influences the material's dielectric response and overall conductivity [10]. At low frequencies, elevated ln εi values indicate space-charge accumulation and electrode polarization at the electrode-electrolyte interface. This behavior is driven by the applied electric field, which causes ion migration and accumulation. Changes in the direction of the electric field occur more quickly at higher frequencies. This is why most ions remain in a static condition; electrode polarization decreases as a result. The frequency sweeping's power-law suggests that there is abnormal charge diffusion present. The conductivity and permittivity of ion-conducting materials affect this occurrence. According to a few reports, the high-frequency region contains the allowable frequency variation. [11, 12].

According to Funke et al. [13] Ion dynamics and conductivity profiles are influenced by the polymer matrix, which promotes ion transport. Their results show that well-established models can represent the frequency-dependent conductivity of polymer-based electrolytes. The confinement of charge carriers within the polymer network is responsible for the observed dispersion in conductivity at high frequencies. This phenomenon illustrates how ionic mobility and polymer chain dynamics interact.

Figure 4 illustrates the relationship between the exponent (s) value and temperature in the SBPEs system. The temperature dependence of the exponent values can provide insights into the system's conduction mechanism, which can be analyzed using various theoretical models. One such model is the Quantum Mechanical Tunneling (QMT) theory, which suggests that charge carriers tunnel through potential barriers without requiring thermal activation. According to the Quantum Mechanical Tunneling (QMT) model, the s value remains temperature-independent [22], suggesting that conduction occurs primarily through tunneling mechanisms rather than thermally assisted hopping.

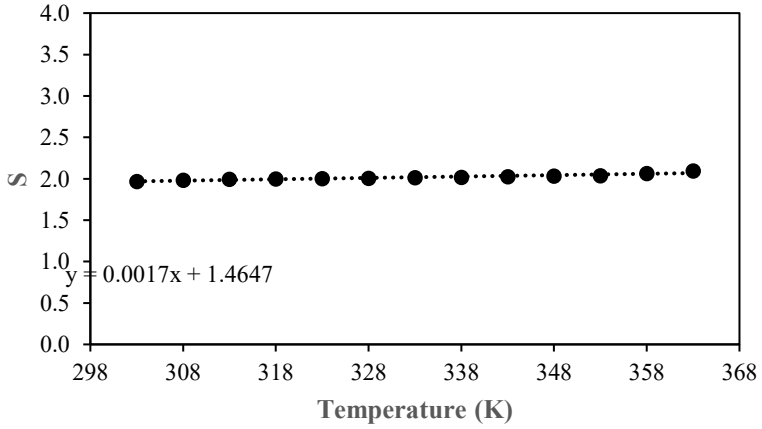

Figure 4. Plot of exponent *s* value against temperature.

In contrast, the Correlated Barrier Hopping (CBH) model predicts that as the temperature (T) approaches 0 K, the s value decreases towards unity [23]. This implies that at lower temperatures, charge carriers require lower activation energy to hop between localized states, influencing the conduction process. On the other hand, the Small-Polaron Hopping (SPH) model suggests that *s* increases with rising temperature [24], indicating that higher thermal energy enhances polarons' ability to overcome potential barriers, thereby facilitating charge transport. Based on Figure 5. the exponent *s* is almost similar at the elevated temperature, suggesting that the conduction mechanism of the SBPEs system can be modelled according to the QMT model. For QMT, the polarons are composed of free ions that migrate and their associated thresholds. This polaron can tunnel through the potential barrier when NH_4SCN is incorporated into the system, which contains a carboxylate functional group and a hydroxyl group. [14]. Shukur et al. [25] stated that the QMT going through the ionic hopping between two complexation sites just not only occurs by crossing over a barrier. Also, an electric field was applied at the selected frequency, pushing the charge carriers to move rapidly over a shorter distance across the entire temperature range. Notably, the plot can be described and fitted by the equation $s = 0.0017x + 1.4647$.

Dielectric Studies

Understanding and evaluating the conductivity and performance of SBPEs and other polymer electrolytes requires ε_r (dielectric permittivity) studies, which provide deeper insights into conductivity trends. These studies also offer crucial information on the polarization effect at the electrode-electrolyte interface, which plays a significant role in charge transport and overall system efficiency [26]. The real part of permitivity ε_r, corresponds to the materials ability to stored charges, while the imaginary part ε_i represents the energy loss due to ion movement and dipole alignment as the electric field rapidly changes direction [27]. From the impedance study real and imaginary components, the ε_r and ε_i plotting graph were calculated using equations (5) and (6):

$$\boldsymbol{\varepsilon_r} = \frac{Z_i}{\omega C_\circ (Z_r^2 + Z_i^2)} \tag{5}$$

$$\boldsymbol{\varepsilon_i} = \frac{Z_r}{\omega C_\circ (Z_r^2 + Z_i^2)} \tag{6}$$

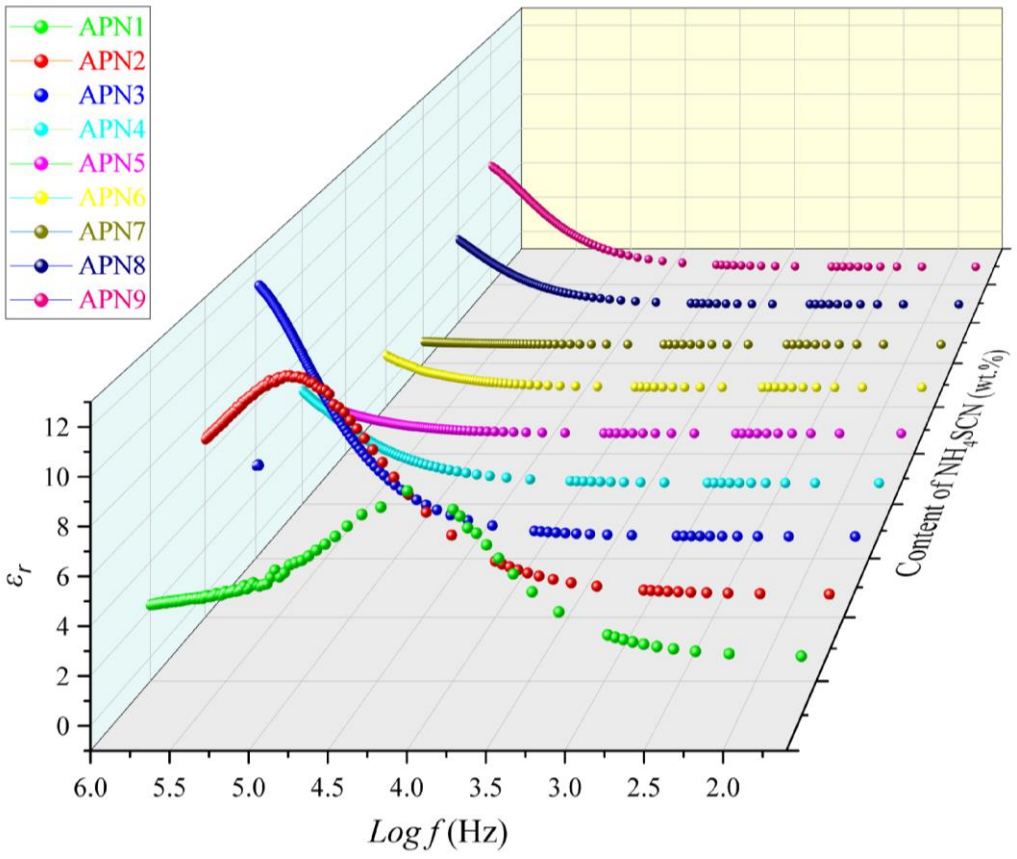

Figure 5. ε_r against Log f (Hz) of SBPEs with various composition of NH_4SCN.

The complex permittivity ε can be used to define the frequency-dependent parameters that characterize the dielectric properties of any system. The complex permittivity or dielectric constant of a system is defined by $\varepsilon = \varepsilon_r - \varepsilon_i$. The real and imaginary parts of complex permittivity are of particular significance for an ion-conducting polymer. Figure 5 (a) and 6 (a) illustrate the relationship between the ε_r and ε_i of the Alg-PVA-NH_4SCN SBPEs system at ambient temperature, as it fluctuates with frequency. The loss tangent (tan δ) is the ratio of the imaginary part (energy loss component, ε_i) to the real part (energy storage component, ε_r) of the material's complex permittivity. Initially, the loss increases with rising frequency, reaching a maximum at a specific frequency (where $\omega\tau = 1$) after which it decreases at high frequency [28]. The observed high values of ε_r and ε_i at low frequency in Figure 5 and 6 can be attributed to electrode polarization phenomena. These phenomena result in the accumulation of charge carriers at the interface between the electrode and electrolyte, leading to a non-Debye behaviour characterized by the absence of a single relaxation time. This deviation from ideal Debye relaxation arises from the structural and dynamic heterogeneity within the polymer electrolyte system. In the Alg–PVA–NH_4SCN matrix, ions experience a broad distribution of local environments and potential energy barriers due to varying degrees of ion–polymer coordination and segmental mobility. As a result, different charge carriers relax at different rates rather than following a uniform relaxation process. The coexistence of free ions, ion pairs, and clusters, together with the amorphous and semi-crystalline regions of the polymer blend, contributes to this distributed relaxation time. Consequently, the overall dielectric response reflects a superposition of multiple relaxation mechanisms, giving rise to the observed non-Debye behaviour [19, 20].

Electrode polarization is strongly influenced by the polymer matrix structure and the nature of ion–polymer interactions. The Alg-PVA blend provides flexible coordination sites, such as hydroxyl and carboxyl groups, which facilitate ion dissociation and mobility[21]. The introduction of NH_4SCN enhances the availability of mobile ions; however, excessive salt content can lead to ionic aggregation and reduced segmental motion of the polymer chains. These structural constraints hinder the reorientation of dipoles and restrict charge transport, thereby affecting both εr and εi value. The samples with moderate NH_4SCN content (APN7) demonstrate an optimal balance of charge mobility, while excessive salt content (APN8 and APN9) exhibits reduced energy dissipation, likely due to ion clustering and restricted mobility[29].

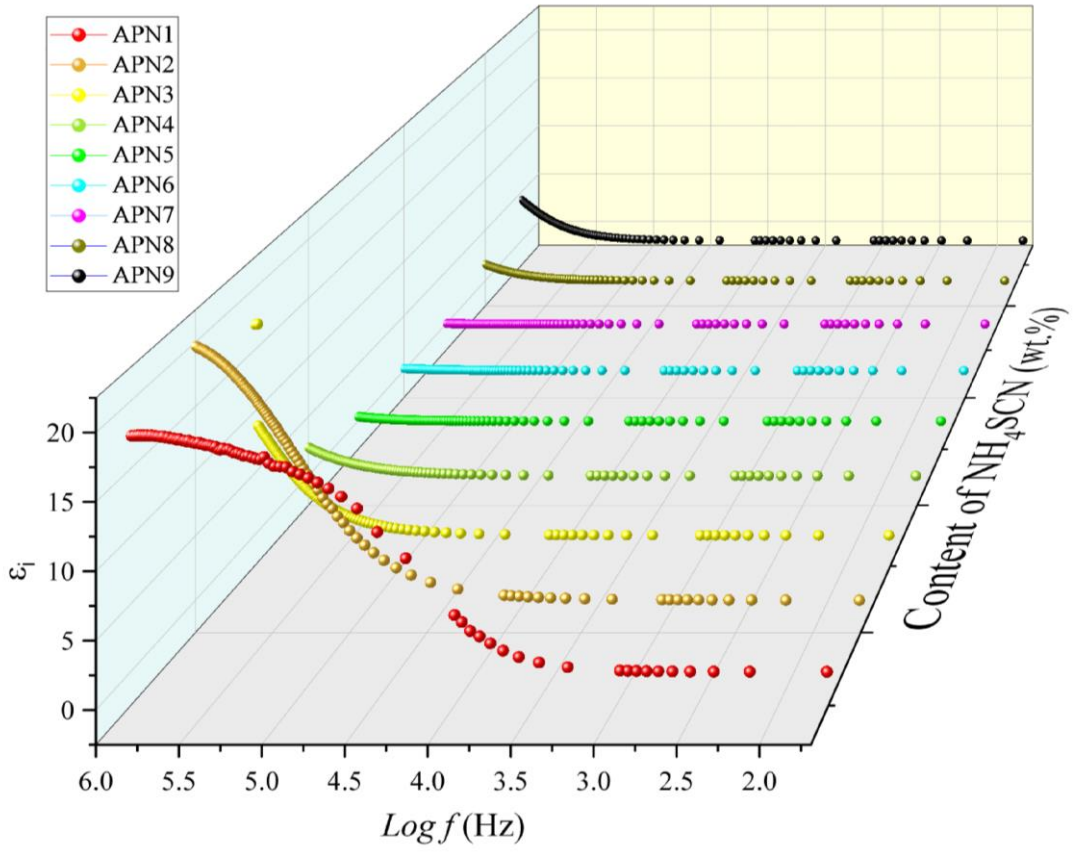

Figure 6. ε_i against Log f (Hz) of SBPEs with various composition of NH_4SCN.

Electric Modulus Analysis at Ambient Temperature

The electrical moduli of real modulus and imaginary modulus revealed a characteristic where plateau region at lower frequency and the curve is increasing at higher frequency, indicating the accumulation activities of charge close to the electrode, commonly referred to as electrode polarization, also causes a significant permittivity [7]. The phenomenon of electrode polarization affects the relaxation process, as evidenced by the modulus study. In this context, the use of M_r is defined as the inverse of permittivity ε_r and provides critical insight. M_r has widely employed to analyze conductivity relaxation behavior of polymer electrolytes as it effectively eliminates the influence of electrode polarization, offering a clearer and more accurate representation of the material's electrical properties [30]. From the ε, real (M_r) and imaginary (M_i) modulus are calculated using the equations (7 and 8) [31], [32], [33]:

$$M_r = \frac{\varepsilon_r}{\varepsilon_r{}^2+\varepsilon_i{}^2} \quad (7)$$

$$M_i = \frac{\varepsilon_i}{\varepsilon_r{}^2+\varepsilon_i{}^2} \quad (8)$$

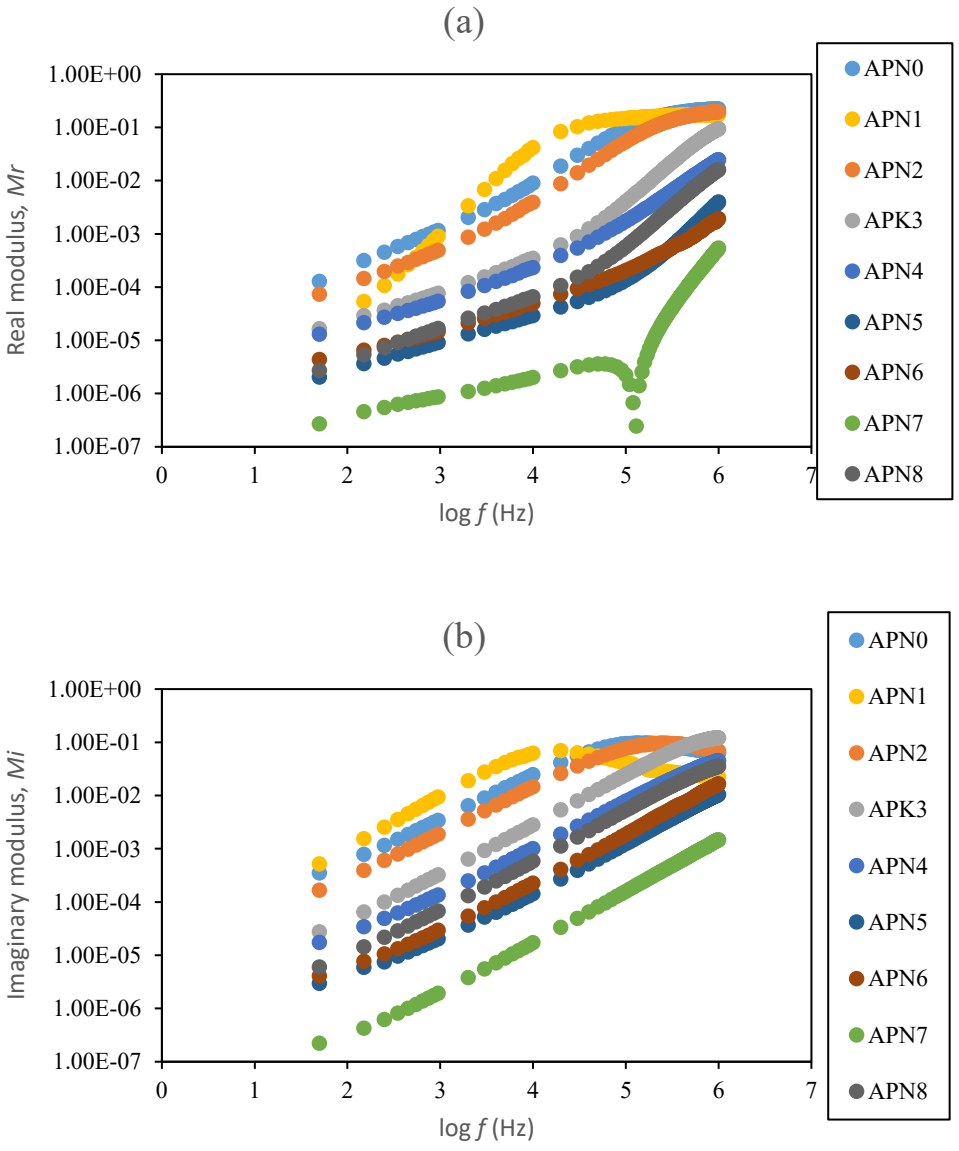

Figure 7. (a) Plot of Real part of Modulus. (b) Plot of Imaginary part of Modulus.

Figure 7 depicts the frequency-dependent behaviour of the real and imaginary parts of the electric modulus, abbreviated as M_r and M_i, respectively. Modulus analysis is important and provides insight into the relaxation behaviour and ion dynamics within the polymer matrix. Both figures emphasize the bulk properties while reducing the influence of electrode polarization. Figure 6(a) and (b) present the M_r and M_i of the electric modulus against *log f* with respect to the various compositions of the salt content, where the graphs display a substantial decline in strength with an increase in salt concentration.

Notably, the M_r values are continuously small, at low frequencies, which can be ascribed to the system's large capacitance [34]. The ions may easily migrate within the polymer matrix under the supplied electric field at low frequencies, enabled by this high capacitance. M_r increases in frequency, especially for samples with increasing NH_4SCN content. It indicates that the synthesized SBPEs are good ionic conductors by the presence of the peak curve in the M_r at higher frequencies [35]. These frequencies cause a decrease in ionic conduction and an increase in modulus because the charge carriers cannot keep up with the electric field's rapid oscillations. This behavior points to the onset of relaxation processes, in which ion hopping is inhibited as the polymer matrix stiffens.

Such relaxation behavior is strongly governed by the microstructure of the Alg–PVA matrix and the extent of ion–polymer coordination. The flexible PVA chains and carboxylate groups of alginate serve as coordination centers for NH_4^+ and SCN^- ions, enabling efficient ion migration at low frequencies. As the salt concentration increases, stronger ion–dipole interactions and partial ionic aggregation occur, restricting polymer chain mobility and segmental motion[5]. This results in a stiffer polymer backbone, limiting ion hopping and dipole reorientation at higher frequencies, which corresponds to the observed increase in M_r and the onset of relaxation. It is noted that the high-frequency region corresponds to the maximum saturation level of Mr. At high frequencies, the Mr value decreases, and thus M_r reaches its maximum value ($M\infty = 1/\varepsilon\infty$). A dispersion in Mr is observed as the frequency is increased, indicating the non-Debye behaviour of the SBPEs system [36].

CONCLUSION

In this present work, different compositions of NH_4SCN have been incorporated in Alg-PVA polymer matrix by solution casting. The complex permittivity, electrical conductivity, and modulus formalism provide better insight of ion dynamics. The sample was characterized by using electrical impedance spectroscopy. The high dielectric constant was observed for the 12 wt.% concentration, which means the highest ionic conductivity. Non-Debye type relaxation is anticipated based on the asymmetrical peak form of ε_r, ε_i, M_r, and M_i. It was found that the AC conductivity of Alg-PVA doped with 35 wt.% NH_4SCN follows the Quantum Mechanical Tunnelling (QMT) model, where charge carriers tunnel through the potential barrier, and the s value remains temperature-independent. This indicates that conduction occurs primarily through tunnelling rather than thermally activated hopping. Therefore, dielectric studies serve as an effective approach for investigating the charge-transport mechanism and dielectric relaxation in electrolyte materials, providing valuable insights into their electrical properties and performance.

ACKNOWLEDGEMENTS

The authors would like to thank Ministry of Higher Education Malaysia (MOHE) under the FRGS fund (FRGS/1/2023/STG05/UMP/02/2) and University Malaysia Pahang Al-Sultan Abdullah (UMPSA) under the UMPSA Distinguished Grant (RDU233001) for funding this research, for the help and support given for the completion of this work. The authors would also like to thank Ionic Materials Team members for kindly help in completing this research.

REFERENCES

1. Arya, A. & Sharma, A. L. (2018) Effect of salt concentration on dielectric properties of Li-ion conducting blend polymer electrolytes. *Journal of Materials Science: Materials in Electronics*, **29(20)**, 17903–17920.

2. Abdulkadir, B. A., Dennis, J. O., Abd Shukur, M. F. B., Nasef, M. M. E. & Usman, F. (2021) Study on dielectric properties of gel polymer electrolyte based on PVA-K2CO3 composites. *International Journal of Electrochemical Science*, **16(1),** 150296.

3. Verma, M. L. & Sahu, H. D. (2017) Study on ionic conductivity and dielectric properties of PEO-based solid nanocomposite polymer electrolytes. *Ionics*, **23(9)**, 2339–2350.

4. Arya, A. & Sharma, A. L. (2018) Structural, electrical properties and dielectric relaxations in Na^+-ion-conducting solid polymer electrolyte. *Journal of Physics: Condensed Matter*, **30(16)**, 165402.

5. Ghazali, N. M., Fuzlin, A. F., Saadiah, M. A., Hasan, M. M., Nagao, Y. & Samsudin, A. S. (2022) Studies on H^+ ions conducting bio-polymer blend electrolyte based on alginate-PVA doped with NH_4NO_3. *Journal of Non-Crystalline Solids*, **598**, 121939.

6. Abdulkadir, B. A., Dennis, J. O., Adam, A. A., Al-Dhahebi, A. M. & Shukur, M. F. (2022) Novel electrospun separator-electrolyte based on PVA-K_2CO_3-SiO_2-cellulose nanofiber for application in flexible energy storage devices. *Journal of Applied Polymer Science*, **139(23),** 52308.

7. Koduru, H. K., Marino, L., Scarpelli, F., Petrov, A. G., Marinov, Y. G., Hadjichristov, G. B. & Scaramuzza, N. (2017) Structural and dielectric properties of NaIO4–complexed PEO/PVP blended solid polymer electrolytes. *Current Applied Physics*, **17(11)**, 1518–1531.

8. Liew, C. W., Ramesh, S., Ramesh, K. & Arof, A. K. (2012) Preparation and characterization of lithium ion conducting ionic liquid-based biodegradable corn starch polymer electrolytes. *Journal of Solid State Electrochemistry*, **16(5),** 1869–1875.

9. Jonscher, A. K. (1977) The 'universal'dielectric response. *Nature*, **267(5613)**, 673–679.

10. Rayssi, C., Kossi, S. E., Dhahri, J. & Khirouni, K. (2018) Frequency and temperature-dependence of dielectric permittivity and electric modulus studies of the solid solution $Ca_{0.85}Er_{0.1}Ti_{1-x}Co_{4x/3}O_3$ ($0 \leq x \leq 0.1$). *Rsc Advances*, **8(31)**, 17139–17150.

11. Sohaimy, M. I. H. & Isa, M. I. N. (2017) Ionic conductivity and conduction mechanism studies on cellulose based solid polymer electrolytes doped with ammonium carbonate. *Polymer Bulletin*, **74(4)**, 1371–1386.

12. Shukla, N., Thakur, A. K., Shukla, A. & Marx, D. T. (2014) Ion conduction mechanism in solid polymer electrolyte: an applicability of almond-west formalism. *International Journal of Electrochemical Science*, **9(12)**, 7644–7659.

13. Zhang, Z., Krishna, R., Zofchak, E. S., Marioni, N., Sachar, H. S. & Ganesan, V. (2023) The influence of counterion structure identity on conductivity, dynamical correlations, and ion transport mechanisms in polymerized ionic liquids. *The Journal of Chemical Physics*, **159(8)**.

14. Isa, M. I. N. & Samsudin, A. S. (2013) Ionic conduction behavior of CMC based green polymer electrolytes. *Advanced Materials Research*, **802**, 194–198.

15. Shukur, M. F., Ibrahim, F. M., Majid, N. A., Ithnin, R. & Kadir, M. F. Z. (2013) Electrical analysis of amorphous corn starch-based polymer electrolyte membranes doped with LiI. *Physica Scripta*, **88(2)**, 025601.

16. Yusof, Y. M., Shukur, M. F., Illias, H. A. & Kadir, M. F. Z. (2014) Conductivity and electrical properties of corn starch–chitosan blend biopolymer electrolyte incorporated with ammonium iodide. *Physica Scripta*, **89(3)**, 035701.

17. Khalil, A. S., Jawad, M. K., Alsammarraie, A. M. & Jaafar, H. I. (2017) Effect of SiO_2 Nanoparticles on Some Mechanical Properties of Epoxy/MWCNT Composites. *Asian Journal of Chemistry*, **29(3)**, 675.

18. Rajeswari, N., Selvasekarapandian, S., Sanjeeviraja, C., Kawamura, J. & Asath Bahadur, S. (2014) A study on polymer blend electrolyte based on PVA/PVP with proton salt. *Polymer bulletin*, **71(5),** 1061–1080.

19. Ramesh, S. & Arof, A. K. (2001) Ionic conductivity studies of plasticized poly (vinyl chloride) polymer electrolytes. *Materials Science and Engineering: B*, **85(1)**, 11–15.

20. Macdonald, J. R. & Johnson, W. B. (2018) Fundamentals of impedance spectroscopy. *Impedance Spectroscopy: Theory, Experiment, and Applications*, 1–20.

21. Ghazali, N. M., Mazuki, N. F. & Samsudin, A. S. (2021) Characterization of biopolymer blend-based on alginate and poly (vinyl alcohol) as an application for polymer host in polymer electrolyte. In *IOP Conference Series: Materials Science and Engineering*, **1092(1)**, 012047.

22. Ahmed, H. T. & Abdullah, O. G. (2020) Structural and ionic conductivity characterization of PEO: MC-NH_4I proton-conducting polymer blend electrolytes-based films. *Results in Physics*, **16**, 102861.

23. Aziz, S. B., Abdullah, O. G., Hussein, S. A. & Ahmed, H. M. (2017) Effect of PVA blending on structural and ion transport properties of CS: AgNt-based polymer electrolyte membrane. *Polymers*, **9(11)**, 622.

24. Karmakar, A. & Ghosh, A. J. C. A. P. (2012) Dielectric permittivity and electric modulus of polyethylene oxide (PEO)–LiClO4 composite electrolytes. *Current Applied Physics*, **12(2),** 539–543.

25. Dave, G. & Kanchan, D. (2018) Dielectric relaxation, and modulus studies of PEO-PAM blend based sodium salt electrolyte system. *Indian Journal of Pure & Applied Physics (IJPAP)*, **56(12),** 978–988.

26. Pawlicka, A., Tavares, F. C., Dörr, D. S., Cholant, C. M., Ely, F., Santos, M. J. L. & Avellaneda, C. O. (2019) Dielectric behavior and FTIR studies of xanthan gum-based solid polymer electrolytes. *Electrochimica Acta*, **305**, 232–239.

27. Aziz, S. B., Brza, M. A., Hamsan, M. H., Kadir, M. F. Z., Muzakir, S. K. & Abdulwahid, R. T. (2020) Effect of ohmic-drop on electrochemical performance of EDLC fabricated from PVA: dextran: NH_4I based polymer blend electrolytes. *Journal of Materials Research and Technology*, **9(3),** 3734–3745.

28. Salman, Y. A., Abdullah, O. G., Hanna, R. R. & Aziz, S. B. (2018) Conductivity and electrical properties of chitosan-methylcellulose blend biopolymer electrolyte incorporated with lithium tetrafluoroborate. *International Journal of Electrochemical Science*, **13(4)**, 3185–3199.

29. Shekhar, M., Pradhan, L. K., Kumar, L. and Kumar, P. (2023) Dielectric Relaxation Behavior and Conduction Mechanism of Ca and Ti Co-Doped Multiferroic Bismuth Ferrite. *J. Electron Mater*, **52**, 9.

30. Aziz, S. B., Abdullah, O. G., Hussein, S. A. & Ahmed, H. M. (2017) Effect of PVA blending on structural and ion transport properties of CS: AgNt-based polymer electrolyte membrane. *Polymers*, **9(11)**, 622.

31. Karmakar, A. & Ghosh, A. J. C. A. P. (2012) Dielectric permittivity and electric modulus of polyethylene oxide (PEO)–$LiClO_4$ composite electrolytes. *Current Applied Physics*, **12(2)**, 539–543.

32. Dave, G. & Kanchan, D. (2018) Dielectric relaxation and modulus studies of PEO-PAM blend based sodium salt electrolyte system. *Indian Journal of Pure & Applied Physics (IJPAP)*, **56(12)**, 978–988.

33. Pawlicka, A., Tavares, F. C., Dörr, D. S., Cholant, C. M., Ely, F., Santos, M. J. L. & Avellaneda, C. O. (2019) Dielectric behavior and FTIR studies of xanthan gum-based solid polymer electrolytes. *Electrochimica Acta*, **305**, 232–239.

34. Aziz, S. B., Brza, M. A., Hamsan, M. H., Kadir, M. F. Z., Muzakir, S. K. & Abdulwahid, R. T. (2020) Effect of ohmic-drop on electrochemical performance of EDLC fabricated from PVA: dextran: NH_4I based polymer blend electrolytes. *Journal of Materials Research and Technology*, **9(3)**, 3734–3745.

35. Salman, Y. A., Abdullah, O. G., Hanna, R. R. & Aziz, S. B. (2018) Conductivity and electrical properties of chitosan-methylcellulose blend biopolymer electrolyte incorporated with lithium tetrafluoroborate. *International Journal of Electrochemical Science*, **13(4)**, 3185–3199.

36. Shekhar, M., Pradhan, L. K., Kumar, L. & Kumar, P. (2023) Dielectric relaxation behavior and conduction mechanism of Ca and Ti co-doped multiferroic bismuth ferrite. *Journal of Electronic Materials*, **52(9)**, 6182–6202.